J. Fluid Mech. (1970), *vol.* 44, *part* 4, *pp.* 673–693
Printed in Great Britain

Convection in an internally heated layer

By R. THIRLBY
School of Mathematics, University of Newcastle upon Tyne

(Received 23 August 1969 and in revised form 2 April 1970)

A numerical study has been made of steady laminar convection in an infinite horizontal layer of fluid, bounded above by a rigid plate held at constant temperature, and below by a thermal insulator. The fluid is heated by a uniform distribution of heat sources. Recent methods for the solution of the Navier–Stokes equations by finite differences are discussed, and the results of integrations in two and three space dimensions and time are presented in an attempt to determine the planform and other flow properties as functions of the Rayleigh and Prandtl numbers.

These results are compared with a preliminary study by Roberts (1967) using a mean-field equation approach and with experimental observations by Tritton & Zarraga (1967) and Hooper (private communication).

1. Introduction

This paper deals with the convective motions which can arise in an infinite layer of homogeneous fluid between fixed horizontal planes, when heated sufficiently strongly from within by a uniform distribution of heat sources. The lower boundary is assumed to be thermally insulating and the upper to be perfectly conducting and maintained at constant temperature. This situation will be compared with the more familiar Bénard convection, in which the motions are driven by a sufficiently large temperature difference across the layer and not by internal heating. (The lower boundary there is perfectly conducting.) The behaviour of both models is determined by two dimensionless numbers: a Rayleigh number, R, and the Prandtl number P. In both cases a static conduction solution exists which is stable to infinitesimal disturbances for all R less than a certain critical value R_c, which is independent of P. The questions that can be asked about the character of the motion which occurs for $R > R_c$ are similar: Are the motions tessellated? If so, what determines the pattern of periodicity (the preferred planform) and its horizontal wavelength, λ (or equivalently its basic wave-number a)? Do the observed patterns depend on the history of the motion (hysteresis effects)? Recognizing that in the experimental work the layer is bounded in its horizontal extent, under what circumstances does the flow structure depend noticeably on the assumed distant, vertical walls? There is also the possibility that stable finite amplitude solutions exist for $R < R_c$. Such motions have been observed by Rossby (1969) in an experimental study of Bénard convection with rotation, and also by Krishnamurti (1968). The latter work is particularly interesting in that it considers a variant of Bénard

convection with time-varying boundary temperatures with governing equations which are similar to those of the internally heated situation, except for one boundary condition on temperature.

In Bénard convection it is of interest to observe the behaviour of the Nusselt number, N, as a function of R. In the present situation, N, the dimensionless heat flux per unit area, is by definition unity. A similar, equally significant, number here (which is identically unity in the Bénard case!) is

$$M = \frac{\text{mean temperature difference across the layer, no motion}}{\text{mean temperature difference with convection}}.$$

This is the reciprocal of the quantity M defined by Roberts (1967), and has been adopted for the largely aesthetic reason that M then increases from unity with increasing R. The form of the dependence of M on R and other parameters will be considered, and also whether any tendency can be detected for the motions to maximize M.

It should not be thought that the situation considered here is merely another variant of the Bénard configuration: it has considerable interest in its own right. First, the symmetry of the Boussinesq version of the classical Bénard equations makes it in some sense special (see, for example, Schlüter, Lortz & Busse 1965). By adding extra physical effects such as temperature variation of viscosity (Segel & Stuart 1962) or surface tension (Pearson 1958) this symmetry is removed, but at the expense of the introduction of an additional dimensionless parameter. The present situation is inherently asymmetric. Secondly, this configuration is a more faithful (though admittedly still idealized) model of a number of geophysical and meteorological situations than is Bénard convection. For example, convection in the earth's mantle is produced by radioactive heating. Thirdly, there appears to be a real conflict between theory (Roberts 1967) and experiment (Tritton & Zarraga 1967; Hooper, private communication). Roberts's technique was to Fourier analyze the Boussinesq equations in the horizontal plane and then to retain only those terms which define the fundamental planform of the motion. The resulting ordinary differential equations in the vertical co-ordinate admit three distinct types of solution: rolls, hexagons with downward flow at their centres, and hexagons with upward flow at their centres. The latter proved to be always unstable. Down hexagons were found to be stable if R exceeded a Prandtl-number-dependent value R_h, say, and a lay between Prandtl-number-dependent limits. For water with $P = 6{\cdot}7$, R_h was about 8750. Roberts's roll solutions were marginally stable for all values of R at a particular wave-number which increased gradually with R. Tritton & Zarraga's experiments were performed with a fluid of Prandtl number about 5·5 and confined to values of R greater than about 11,000. They observed polygonal cells with downward central motion, the patterns being mainly hexagonal at moderate values of R. Their most striking observation was that the size of these cells increased strongly with increasing R, being four times larger at $R \sim 110{,}000$ than at $R \sim 11{,}000$. The wave-numbers of such solutions were consistently outside the stable range as calculated by Roberts. Hooper's results cover the whole range of R from below R_c upwards. He found only polygonal cells with downward motion at their centres and

reports some elongation of cells with increased R but not on the scale of Tritton & Zarraga's results. The primary objectives of this paper are first to solve the full partial differential equations governing this motion, rather than the use of Roberts's approximate technique, and secondly to shed some light on the obvious discrepancies in the above results.

It is, perhaps, relevant at this point to note the scope and limitations of this approach. The simulation of an infinite layer on a computer is as impractical as it is in the laboratory. It is, however, possible to provide periodic numerical solutions for an infinite layer, by applying cyclic conditions on the appropriate walls. The positions assigned to these walls will determine a basic wavelength, λ, for the ensuing motions. If the volume so constructed is filled by a single cell, we may learn something of the preferred planform, but nothing of the preferred wave-number, or of Fourier modes with wavelengths greater than λ—the so-called subharmonics. If λ is sufficiently large, however, we may expect the volume to contain several cells, and thus study both the subharmonics and the preferred wave-number. The information so obtained is incomplete since it does not, unless λ is unpredictably large, decide the preferred a within narrow limits. In principle this difficulty can be overcome by the method developed by Schlüter *et al.* (1965) and extended by Busse (1967*a*, *b*). In this, the unit cell is imagined repeated to infinity and subjected to a perturbation whose periodicity need not be an integral multiple of a. The resulting problem for the perturbation is cast in a form which depends only on the basic cell of the steady solution. Assuming that, indeed, a preferred mode of a single periodicity does exist, this is probably the only satisfactory way of finding it. This paper does not attempt to answer questions of this type, but in the limited case of two-dimensional flow some estimate of the preferred period was obtained by making λ so large that 30–40 cells were observed.

The results so obtained support Roberts's view that the preferred wave-number increases as R is increased. In three dimensions such an approach was not possible with the computing power available. The single cell results for $P \sim 6$ suggest that some kind of three-dimensional flow is always possible and that the planform will be hexagonal with downward central flow at least for R greater than 15,000.

2. The model equations: the linear theory and its consequences

The basic model consists of a uniform horizontal layer $0 < z < d$, unbounded in the x and y directions and containing a fluid of density ρ, kinematic viscosity ν, thermal diffusivity κ and coefficient of volume expansion α. The layer is heated internally in such a way that, in the absence of conduction, the temperature of each fluid element would rise at a constant rate γ. To define a set of non-dimensional variables the following scales are used; time, t, in units of d^2/ν; length in units of d; velocity, $\mathbf{u}$, in units of ν/d; and temperature, T, from zero at the upper surface, in units of $\gamma d^2/\kappa$. The Prandtl and Rayleigh numbers are defined by

$$P = \nu/\kappa, \quad R = \alpha\gamma g d^5/\nu\kappa^2,$$

where g is the acceleration due to gravity. In component form, we write $\mathbf{u} = (u, v, w)$. The basic equations then become, in the Boussinesq approximation,

$$\operatorname{div} \mathbf{u} = 0, \tag{1}$$

$$\partial \mathbf{u}/\partial t + \mathbf{u} \,.\, \operatorname{grad} \mathbf{u} = -\operatorname{grad} \pi + \nabla^2 \mathbf{u} + (R/P)\, T' \mathbf{k}, \tag{2}$$

$$P(\partial T'/\partial t + \mathbf{u} \,.\, \operatorname{grad} T') = \nabla^2 T' + 1. \tag{3}$$

Here π is a non-dimensional pressure variable, and $\mathbf{k}$ is a unit vector in the upward (i.e. z increasing) direction. The relevant boundary conditions, assuming rigid no-slip surfaces, are

$$\partial T'/\partial z = 0 \quad \text{and} \quad \mathbf{u} = 0, \quad \text{on} \quad z = 0, \tag{4}$$

$$T' = 0 \quad \text{and} \quad \mathbf{u} = 0, \quad \text{on} \quad z = 1. \tag{5}$$

Steady 'conduction' solutions exist in which

$$\mathbf{u} = 0, \quad T' = T'^{(0)}(z) = \tfrac{1}{2}(1 - z^2), \quad \pi = \pi^{(0)}(z) = (R/P)\,(c + \tfrac{1}{2}z - \tfrac{1}{6}z^3), \tag{6}$$

and c is an arbitrary constant. If R is sufficiently large, steady 'convection' solutions are also found with

$$\mathbf{u} \neq 0, \quad T' = T_0(z) + \theta(x, y, z), \quad \pi = \pi_0(z) + \Pi(x, y, z), \tag{7}$$

in which the averages $\langle \mathbf{u} \rangle$, $\langle \theta \rangle$ and $\langle \Pi \rangle$ of $\mathbf{u}$, θ and Π over any horizontal plane are zero. Here the functions $\mathbf{u}$, θ and Π represent the tessellated motions of convection and T_0 and Π_0 are the corresponding conduction terms $T'^{(0)}$ and $\pi^{(0)}$ as modified by these motions. These quantities can be expanded in sums of terms of the form

$$\mathbf{u} = \left[\frac{DW(z)}{a^2} \frac{\partial f(x,y)}{\partial x}, \quad \frac{DW(z)}{a^2} \frac{\partial f(x,y)}{\partial y}, \quad W(z) f(x,y) \right] \tag{8}$$

and

$$\mathbf{u} = \left[\frac{V(z)}{a^2} \frac{\partial g(x,y)}{\partial y}, \quad -\frac{V(z)}{a^2} \frac{\partial g(x,y)}{\partial x}, \quad 0 \right],$$

which represent the poloidal and toroidal parts of the velocity field respectively; and

$$\theta = F(z) f(x, y), \quad \Pi = G(z) f(x, y),$$

where both $f(x, y)$ and $g(x, y)$ satisfy

$$\frac{\partial^2 f}{\partial x^2} + \frac{\partial^2 f}{\partial y^2} = -a^2 f \quad \text{and} \quad D \equiv \frac{d}{dz}. \tag{9}$$

(See Chandrasekhar 1961, chapter 2.)

For infinitesimal disturbances, the equations governing W, F and G are linear and the individual Fourier modes do not interact. These equations do not in general possess a solution. However, for each a, independent of the choice of f, they pose an eigenvalue problem for R. The smallest eigenvalue $R(a)$, say, has a minimum R_c which corresponds to a wave-number a_c, say. These quantities decide the critical Rayleigh number and wave-numbers at which convection first occurs if R is increased gradually from zero. They were calculated by

Roberts (1967), his values being 2772 and 2·63 respectively. They had been previously estimated by Debler (1966) as 2786 and 2·5. The single wave-number character of the convection patterns that occur at R_c merely reflects the fact that only one mode, a_c, is self-excited. The precise form of tessellation is determined by non-linear effects which cause the modes such as (8) to interact. In particular the mode a excites the higher harmonics $2a$, $3a$, etc. It is possible to use this approach to solve the non-linear convection problems by splitting the partial differential equations into a set of ordinary differential equations for individual Fourier modes and explicitly computing their interactions; see, for example, Ehrenzweig (1969). It should be noted that there is also the possibility of cascade up the spectrum, i.e. of subharmonics being excited. For example, in the case of a roll of wave-number a, this would imply the maintenance of harmonics of wave-number $\frac{1}{2}a$. This effect should be especially important where an infinite layer is approximated by one of finite extent.

Qualitatively correct behaviour of M for small $R-R_c$ in the absence of sub-critical finite amplitude solutions can be readily obtained by applying the 'shape hypothesis' of Stuart (1958). This yields an expression (Roberts 1967) of the form

$$M = \frac{R}{R(1-\Gamma)+\Gamma R(a)}, \tag{10}$$

where Γ is given in terms of the marginal solution for $\mathbf{u}$ and θ for the chosen a by

$$\Gamma = 2\int_0^1 \langle\theta w\rangle\, dz \int_0^1 \langle\theta w\rangle\, z\, dz \Big/ \int_0^1 \langle\theta w\rangle^2\, dz.$$

Taking $a = a_c$ and $R(a) = R_c$, Roberts obtained the value 0·5994 for Γ, and this has been used to obtain the curve shown in figure 1 (labelled 'Roberts, shape assumption').

Only certain types of solution of equation (9) will be of use in this study, the simplest being $f = \cos(ax)$, representing rolls of width π/a with their axes in the y direction. Combining three such sets of rolls mutually inclined at 60°, we have

$$f = \cos(\tfrac{1}{2}\sqrt{3}\,ax + \tfrac{1}{2}ay) + \cos(\tfrac{1}{2}\sqrt{3}\,ax - \tfrac{1}{2}ay) + A\cos(ay), \tag{11}$$

giving a type of closed cell whose importance was first stressed by Segel & Stuart (1962). The geometry of this cell depends on the constant A, and varies between rectangular at $A = 0$ and hexagonal at $A = 1$. Combining the first two terms of (11) produces the equivalent expression

$$f = 2\cos(\tfrac{1}{2}\sqrt{3}\,ax)\cos(\tfrac{1}{2}ay) + A\cos(ay). \tag{12}$$

In this form it is seen that f has periods in the x and y directions of $4\pi/\sqrt{3}a$ and $4\pi/a$, respectively. Three-dimensional solutions will be sought satisfying periodic conditions based on these values.

2.1. *Numerical methods*

Equations (2) and (3), together with the boundary conditions (4) and (5), could be solved for $\mathbf{u}$ and T by standard 'marching' techniques. This unfortunately leaves π to be determined by the only remaining equation, (1), which is π independent.

In the limited case of two-dimensional flow in the (x, z) plane, this problem can be resolved by the introduction of a stream function, ψ, for the velocity. Then taking the curl of equation (2) to eliminate π terms, we have

$$\frac{\partial \xi}{\partial t} = -\left(\frac{\partial \psi}{\partial z}\frac{\partial \xi}{\partial x} - \frac{\partial \psi}{\partial x}\frac{\partial \xi}{\partial z}\right) + \nabla^2 \xi - \frac{R}{P}\frac{\partial T}{\partial x}, \tag{13}$$

where ξ is the vorticity defined by

$$\xi = \nabla^2 \psi, \quad \text{and} \quad \mathbf{u} = \left(\frac{\partial \psi}{\partial z}, 0, -\frac{\partial \psi}{\partial x}\right). \tag{14}$$

Here both ψ and ξ have simple boundary conditions on a rigid wall,

$$\psi = 0 \quad \text{and} \quad \xi = \partial^2 \psi / \partial z^2. \tag{15}$$

This technique has been successfully used by Pearson (1964) and Fromm (1965). In three dimensions this approach is less attractive because the velocity vector potential has no simple boundary conditions. Returning to equations (1) to (3) in terms of the 'primitive variables' $\mathbf{u}$, T and π: by taking the divergence of (2) an elliptical differential equation for π is obtained. This form was used by Harlow & Welch (1965), using one component of equation (2) to provide a boundary equation for π. This method is particularly attractive in the calculation of flows with free surface conditions.

A more satisfactory method for rigid boundaries is that due to Chorin (1967*a*) and subsequently used by Plows (1968) to survey the effects on Bénard convection of varying Prandtl number. Chorin introduces a small compressibility into the continuity equation, replacing (1) by

$$\partial \rho / \partial t = -\operatorname{div} \mathbf{u}. \tag{16}$$

Here ρ is related to π by an 'equation of state' of a particularly simple form,

$$\pi = c^2 \rho, \tag{17}$$

where c is an arbitrary constant playing the role of a sonic velocity. Equation (16) then becomes

$$\partial \pi / \partial t = -c^2 \operatorname{div} \mathbf{u}. \tag{18}$$

Equations (18), (2) and (3) can then be stepped in time until a time-independent solution is obtained; whence $\partial \pi / \partial t = 0$, by definition, and (18) reduces to equation (1). The value of c clearly does not affect the final solution and is chosen to speed convergence. Computing instabilities arise if c is too small which correspond to the flow becoming supersonic, hence c must obey the relation, $|\mathbf{u}|_{\max} < c$. In fact

$$c = 2|\mathbf{u}|_{\max} \tag{19}$$

appears to be the most acceptable in both this and the Bénard problem.

2.2. *A new development of the method of artificial compressibility for two-dimensional flows*

The above methods, when used to obtain steady solutions, use time effectively only as an iteration parameter. This is convenient in the sense that, given a reasonable initial state, such an iteration will almost certainly converge if a

solution exists. It is, however, somewhat inflexible, and the convergence rate is limited by the numerical stability of the chosen time-stepping procedure. In this paper a method will be used which is based on the time-independent form of equations (1) and (3), making use of equation (18) to find π.

Consider, for example, the z component of equation (2); this is, in its time-independent form,

$$\nabla^2 w - \mathbf{u}.\operatorname{grad} w = \frac{\partial \pi}{\partial z} - \frac{R}{P} T. \tag{20}$$

Only periodic, two-dimensional solutions are sought of wavelength λ, hence the region of interest is the rectangle $0 \leqslant z < 1$, $0 \leqslant x \leqslant \lambda$. Superimposing a regular finite difference net with spatial increments Δx and Δz and denoting $u(q\Delta x, r\Delta z)$ by $U(q,r)$, a convenient finite difference form of (20) is

$$D_{xx} w + D_{zz} w = u[q,r] D_x w + w[q,r] D_z w + D_z \pi - (R/P) T[q,r]. \tag{21}$$

Here the finite difference operators D_x, D_z, D_{xx}, and D_{zz} are defined by formulae of the type:

$$D_x u = \frac{1}{2\Delta x}(u[q+1,r] - u[q-1,r])$$

and

$$D_{xx} u = \frac{1}{\Delta x^2}(u[q+1,r] + u[q-1,r] - 2u[q,r]).$$

This equation is now formally solved for the $w(q,r)$ terms occurring on the right-hand side only. Equations for $u(q,r)$ and $T(q,r)$ are readily found by analogous processes, and can be iterated together to find $u(q,r)$, $w(q,r)$ and $T(q,r)$ everywhere on the mesh, provided a suitable iterative form of (1) can be found for $\pi(q,r)$. Such an equation can be obtained from (18) in the form

$$\pi[q,r] = \pi[q,r] - c^2(D_x u + D_z w). \tag{22}$$

On the boundaries, (18) reduces to

$$\partial \pi / \partial t = -c^2 \partial w / \partial z. \tag{23}$$

In this form, it can be used to obtain π on the boundary by a simple modification of (22), dropping the terms in u and replacing the central difference form of the z derivative of w by a suitable forward and backward form on the bottom and top surfaces respectively.

Since the time-independent form of the other equations is used, $c^2\Delta t$ can be regarded as one arbitrary constant and chosen to suit the numerical process, subject to restrictions analogous to (19). In practical tests with this method $c^2\Delta t$ was chosen by experiment; too small a value produces numerical instability, whereas too large a value causes slow oscillatory convergence. The major attraction of this scheme is its high convergence rate. Comparative tests of convergence are notoriously suspect, especially when performed by an interested party. However, a version of this code was modified to solve the equations of Bénard convection with rigid (i.e. no-slip) boundaries and compared with a Dufort–Frankel artificial compressibility programme kindly supplied by Dr Chorin. Over a series of runs with varying Rayleigh number and a grid size of 28×30, the

present method showed a consistent reduction of more than 60 % in the number of iterations required to achieve a given accuracy. An additional advantage is that only one storage field is required for each variable. This is also possible in a two-time-level scheme such as Dr Chorin's, provided suitable conservative finite differences are used for the advection terms, and the buoyancy force is suitably programmed. The equations then split equally into two disconnected meshes, only one of which need be stored at each time level. Chorin (1967*a*, § III*b*) reports a considerable slowing down in convergence rate in the rigid boundary case due to the use of such difference schemes, thus making this idea self-defeating.

2.3. *Three-dimensional methods*

The technique described in § 2.2 is applicable in three space dimensions but the desirability of studying the transitions from one planform to another make the use of a time-dependent method necessary. That used is largely due to Chorin (1967*b*) and was developed from his earlier technique described in § 2.1. Suppose a finite difference grid is defined with increments Δx, Δy and Δz in three space directions, and Δt in time. Denote by $\mathbf{u}(q, r, s)$ the value of $\mathbf{u}$ at the point $(q\Delta x, r\Delta y, s\Delta z)$. An approximate step to time $t = (n+1)\Delta t$ is made using, in place of (2), a finite difference form of

$$\partial \mathbf{u}/\partial t = \nabla^2 \mathbf{u} - (\mathbf{u}.\operatorname{grad})\mathbf{u} - (R/P)\,T\mathbf{k}, \tag{24}$$

and the result of this called (say) $\mathbf{u}^*$. An iteration is now set up to correct $\mathbf{u}^*$ for the effects of neglecting the π terms of (2). This is done by defining a finite difference analogue $Du = 0$, of $\operatorname{div}\mathbf{u} = 0$ on the interior and $\partial w/\partial z = 0$ on the rigid walls, using central differences for the former, and suitable sideways differences on the walls. The iteration is then written as

$$\pi^{n+1,\,1} = \pi^n, \tag{25}$$

$$\pi^{n+1,\,m+1} = \pi^{n+1,\,m} - \mu D\mathbf{u}^{n+1,\,m+1}, \tag{26}$$

$$\mathbf{u}^{n+1,\,m+1} = \mathbf{u}^* - \Delta t \mathbf{G}^m \pi. \tag{27}$$

Here μ is a parameter; $\pi^{n+1,\,m}$ and $\mathbf{u}^{n+1,\,m}$ are successive approximations to π^{n+1} and $\mathbf{u}^{n+1}$; and $\mathbf{G}^m\pi$ is a vector function of $\pi^{n+1,\,m+1}$ and $\pi^{n+1,\,m}$ which tends to a difference form of $\operatorname{grad}\mathbf{u}^{n+1}$ as $|\pi^{n+1,\,m+1} - \pi^{n+1,\,m}|$ tends to zero. The particular form of $\mathbf{G}^m\pi$ is important, and is best illustrated by example. If we apply (26) to the pressure $\pi(q, r, s)$, the result involves the six velocities

$$u^{n+1,\,m+1}(q \pm 1, r, s), \quad v^{n+1,\,m+1}(q, r \pm 1, s) \quad \text{and} \quad w^{n+1,\,m+1}(q, r, s \pm 1).$$

These are obtained by applying (27) repeatedly as

$$u^{n+1,\,m+1}(q+1, r, s) = u^*(q+1, r, s) - (\Delta t/4\Delta x)\,[2\pi^{n+1,\,m}(q+2, r, s) - \pi^{n+1,\,m}(q, r, s) - \pi^{n+1,\,m+1}(q, r, s)], \tag{28}$$

$$u^{n+1,\,m+1}(q-1, r, s) = u^*(q-1, r, s) - (\Delta t/4\Delta x)\,[\pi^{n+1,\,m}(q, r, s) - \pi^{n+1,\,m+1}(q, r, s) - 2\pi^{n+1,\,m}(q-2, r, s)], \tag{29}$$

with similar expressions for the other two pairs, and natural amendments near the walls. These seven linear equations can be readily solved for $(m+1)$th

approximations to the six velocities and pressure at the $(n+1)$th time step. In this iteration μ acts as a relaxation parameter and it can be shown that the process converges for all μ and that an optimum value of μ can be found (see Chorin 1967*b*).

The initial integration to obtain u^* can be performed in many ways. Chorin suggests an alternating direction implicit method due to Samarskiĭ (1963). This is very economical in its use of storage, but proved very inaccurate in use. This was due to the use of the intermediate field values (analogous to u', u'' and u''' defined below) in the calculation of the advection terms, when such values were not reasonable approximations to u^n and u^{n+1}.

After some experiment the method adopted was a central difference, alternating direction implicit method due to Douglas (1962), being a three-dimensional extension of the well-known algorithm of Peaceman & Rachford (1955). Applied to the x component of (2), three intermediate quantities u', u'', u''' are calculated to obtain u^*, as follows:

$$u' = u^n + \Delta t[\tfrac{1}{2}D_{xx}u' + \tfrac{1}{2}D_{xx}u^n + D_{yy}u^n + D_{zz}u^n] - \tfrac{1}{2}u^nD_xu' - \tfrac{1}{2}u^nD_xu^n - v^nD_yu^n - w^nD_zu^n - D_x\pi^n], \tag{30}$$

$$u'' = u' + \tfrac{1}{2}\Delta t[D_{yy}u'' - D_{yy}u^n - v'D_yu'' + v^nD_yu^n], \tag{31}$$

$$u''' = u'' + \tfrac{1}{2}\Delta t[D_{zz}u''' - D_{zz}u^n - w''D_zu''' + w^nD_zu^n], \tag{32}$$

$$u^* = u''' + \Delta tD_x\pi^n. \tag{33}$$

The inclusion of terms in π at the first step (equation (30)) ensures that u', u'', u''' are successive approximations to u. This minimizes errors in the non-linear terms. Two storage fields per variable are required, one to store the u^n values, the other being used successively for u', u'', u''', and u^*.

The algorithm, as described above, enables steady solutions in three dimensions to be obtained over a limited finite difference grid of 12 mesh points in each direction in about 40 min computer time (programmed in Fortran on an IBM 360/65). This time must be contrasted with a time of less than 2 min to find a steady solution for a single cell in two dimensions (with the much finer 32×32 grid!) using the method of § 2.2.

3. Solutions

3.1. *Solutions in two dimensions for* $P = 6{\cdot}8$

The solutions described in this section were confined to a fixed Prandtl number of 6·8. This value should be compared with those of 6·7, 5·5 and 6·6 given by Roberts, Tritton & Zarraga, and Hooper respectively. A series of iterations, using a constant λ of $2\pi/a_c$ ($= \lambda_c$, say, the wavelength of the solution at R_c), was performed for various values of R in the range 3000 to 52,000, initiating each calculation from the appropriate conduction solution (6), slightly perturbed by a sinusoidal temperature disturbance of wave-number a_c. The values of M so obtained are shown in figure 1. The horizontally averaged mean temperature profile with depth was also calculated for each state and some of these are given as figure 2. Figure 1 also gives the values of M obtained by Roberts, both by his

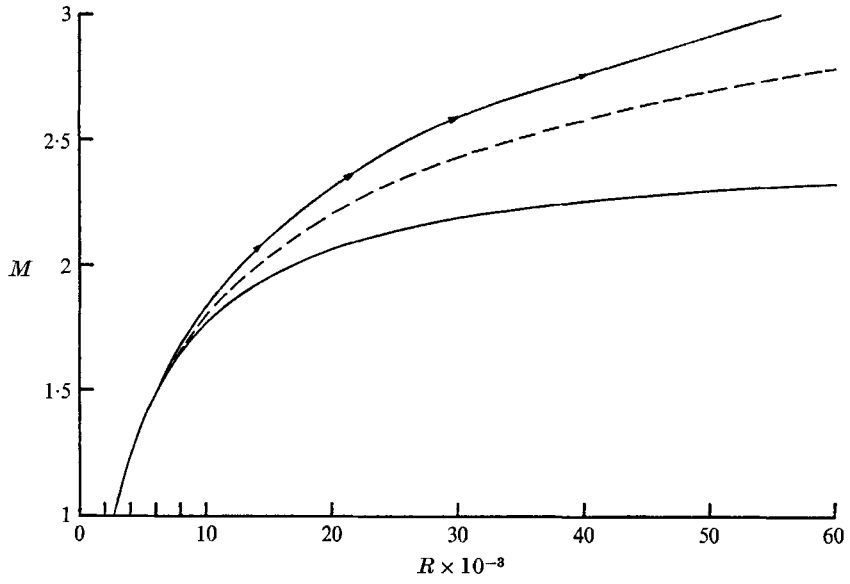

FIGURE 1. M as a function of Rayleigh number R for roll solutions at wave-number a_c. ⟶, Roberts, mean-field; – – –, Thirlby; ——, Roberts, shape assumption.

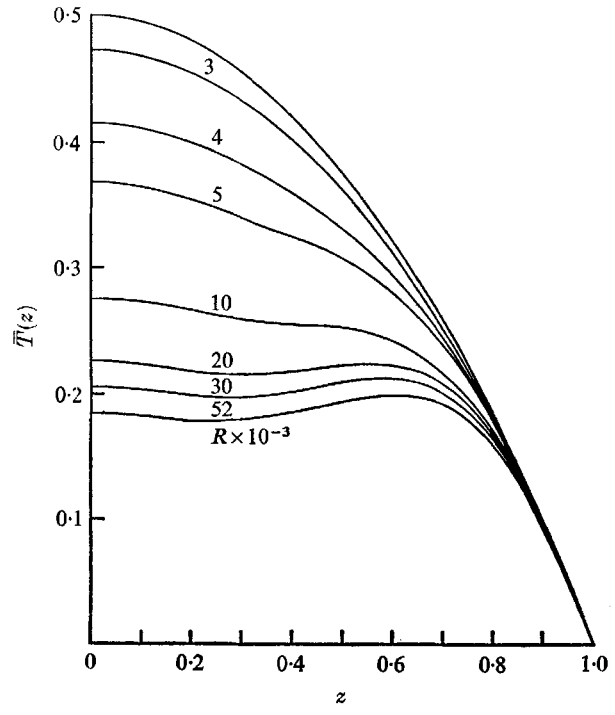

FIGURE 2. Horizontally averaged temperature with depth for roll solutions at wave-number a_0 and various values of R.

non-linear theory and the shape hypothesis. The former are consistently higher due, presumably, to the constraint imposed on the motion implied by his approximation. The agreement between the present results and the shape assumption is remarkably good for R less than about $3R_c$. This may be explained by the parabolic form of the corresponding mean temperature profiles in figure 2. For higher values of R the flow in the lower half of the layer becomes largely isothermal and this 'averaging out' of the profile reduces the lower surface temperature, hence increasing M.

For certain Rayleigh numbers other values of λ were used in the range $\frac{1}{2}\lambda_c$ to $2\lambda_c$. The resulting variation in M was less than 10 % over this range, and M reached a vague maximum near to $\lambda = \lambda_c$. Cells with wavelength greater than $2\lambda_c$ could not be produced—steady states with two or three cells each of proportionately smaller period were observed instead. To permit a greater variety of

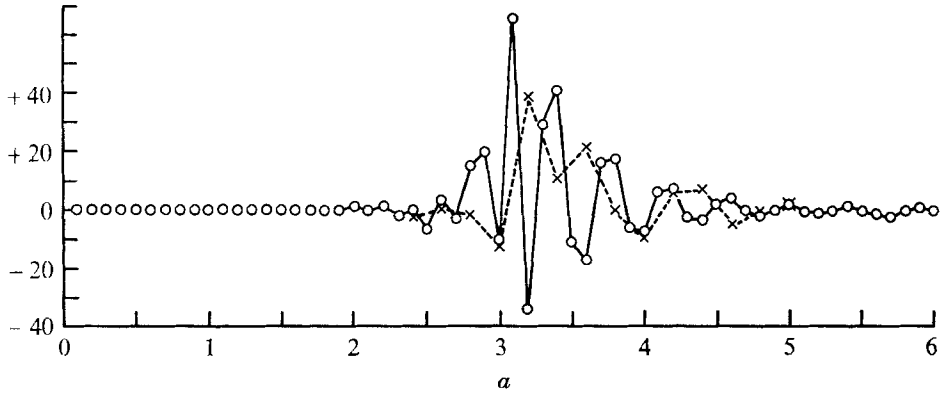

FIGURE 3. Fourier harmonics of two calculations at $R = 10{,}000$, $P = 6{\cdot}8$. --×--, wavelength 10π; —○—, wavelength 20π.

cell sizes to occur, some calculations were carried out with much larger values of λ. With $\lambda = 10\pi$ and $R = 10{,}000$ an initial perturbation in the form of a single roll of wavelength λ produced 17 cells of average wave-number, $\bar{a}$ say, of 3·4. A similar run with $\lambda = 20\pi$ produced 34 cells again with $\bar{a} = 3{\cdot}4$. Fourier analyses of the mid-depth vertical velocity component are given in figure 3. The latter run repeated with 20 % more finite difference points in the horizontal direction again produced 34 cells with a similar, but not identical, Fourier spectrum, as did the result of numerically 'stirring' the above solutions and then reiterating to a steady state. Examination of the Fourier components reveals, first, that only a few wave-numbers contribute much to the motion. These are grouped around the value of $\bar{a}$ and lie in the interval 2·8 to 4·0. This spread of values represents the range of different cell sizes present in these solutions. Secondly, no significant Fourier components are found with wave-numbers corresponding to the natural subharmonics of $\bar{a}$, suggesting that the horizontal extent of the layer is not particularly important in the determination of cell size. Thirdly, and perhaps more surprisingly, the natural overtones of $\bar{a}$ are hardly present. This is in marked contrast to the Fourier spectra of single cell results at similar Rayleigh number,

some of which are given in table 1, normalized so that the value of the fundamental is 100. This casts some doubt on the value of using models which assume only a single cell and its associated overtones. [The variation of the power of the overtone with wave-number in table 1 is to be expected from linear theory. At any particular Rayleigh number $> R_c$, there are two wave-numbers where the motion is marginally stable, and where only one Fourier mode, the fundamental, is self-exciting. Between those values, at which all overtones would have zero amplitudes, they might be expected to increase in power and reach a maximum (hopefully, near to a_c).]

a	1·6	1·8	2·0	2·2	2·4	2·63	2·8	3·0	3·2	3·4	3·6	3·8	4·0
1st	17·9	3·0	5·1	10·0	11·5	12·2	12·0	11·3	10·4	9·5	8·3	6·4	5·5
2nd	30·5	23·0	18·2	14·3	11·6	7·9	6·2	4·8	3·8	2·7	2·1	1·2	0·9

TABLE 1. Amplitudes of the first and second overtones of single roll solutions at $R = 10{,}000$, $P = 6{\cdot}8$, for various wave-numbers. The fundamental has been normalized to 100

l	m	K	M
20	9	1·06	1·88
20	21	1·10	1·86
30	13	1·12	1·85
30	21	1·17	1·81
40	21	1·17	1·81
40	33	1·18	1·80

TABLE 2. Values of M and non-dimensional kinetic energy K for roll solutions at $R = 10{,}000$, $P = 6{\cdot}8$, $a = a_c$ with different finite difference grid sizes. l and m are the numbers of grid points used in the horizontal and vertical directions respectively

The grid size used in the above runs was varied according to Rayleigh number, and, of course, the number of cells present. For single cell calculations at $R < 10{,}000$ a grid size of 20×21 was considered adequate. This was increased with R until at around $R = 52{,}000$ the grid was 40×33 points. An assessment of the errors involved can be made by reference to table 2 which gives the computed values of M for a typical single roll at $R = 10{,}000$ and $a = 2{\cdot}63$ with different grid sizes. Here l is the number of points in the horizontal direction and m the number in the vertical direction. It should be noted that M is consistently overestimated by a coarse grid. This is important in considering the results given in § 3.2. The multicell, $R = 10{,}000$, calculations were performed on grids with $l = 250$ and 300 points and $m = 21$. No appreciable differences were observed between these two sizes; in particular, the number of cells present and the quantity M were not affected. To be reasonably sure of convergence, calculations were continued until the three global quantities M, as previously defined, N the Nusselt number near the upper surface, and K, the total kinetic energy, had all reached steady values to 5 significant figures. (Single precision floating point on the 360/65 is only 24 binary places.) In the multicell calculations some change in cell sizes could still be taking place at this stage, but further iteration did not

appear to change the overall picture very much or show any real sign of all the cells becoming the same size. The actual value of N gives some idea of the conservation of heat in the finite difference approximation, since it should physically be always unity. In practice it did not depart from this by more than 0·5 % in any of the above solutions.

3.2. *Three-dimensional solutions*

Horizontal periods for the three-dimensional calculations were chosen to permit hexagonal solutions. Equation (12) with $A = 1$ for the fundamental mode of a hexagon of wave-number a, has periods $4\pi/\sqrt{3}a$ and $4\pi/a$ in the x and y directions respectively. Defining the basic wavelength λ as $\lambda = 2\pi/a$, these become $2\lambda/\sqrt{3}$ and 2λ (i.e. a rectangle of side ratio $\sqrt{3}$).

Initial values for the integrations were supplied either by superimposing a horizontal perturbation in the form of a hexagon on the temperature field of a conduction solution, or by using the end product of a previous run. The calculation was monitored for values of M and the kinetic energy, and, less frequently, by the display of iso-lines of the vertical velocity component at mid-depth. Using standard values of λ_c, the critical wavelength, and a Prandtl number of 6·8, hexagons with downward motion at their centres, initiated from the conduction solution, became steady after some 6–12 non-dimensional time units, provided R exceeded $\sim$ 15,000. Below this value of R, steady convection was still produced, but the planform varied according to R, from hexagonal at 15,000 to nearly rectangular at critical. In figures 4 (*a*), (*b*), (*c*) and (*d*) the vertical velocity component at mid-depth is shown as a series of contours. The cell boundaries are indicated approximately by the broken lines. The first of these diagrams, at $R = 20{,}000$, may be compared with that given by Chandrasekhar (1961, p. 50).

In table 3 the first few terms of a two-dimensional Fourier analysis of the mid-depth velocity component are given for various Rayleigh numbers. These components were computed from the series

$$f = \sum_{s=0}^{\frac{1}{2}l} \sum_{t=0}^{\frac{1}{2}m} A_{st} \cos(\tfrac{1}{2}\sqrt{3}\, sax) \cos(\tfrac{1}{2}\, tay),$$

where l and m are the numbers of mesh points in the x and y directions respectively. For any particular pair of integers (s, t) the wave-number of the corresponding term is $\frac{1}{2}a(3s^2+t^2)^{\frac{1}{2}}$. The fundamental mode with wave-number a therefore consists of two terms with (s, t) equal to $(1, 1)$ and $(0, 2)$. If the cell is purely hexagonal (12) shows that the ratio of the amplitudes of these terms should be 2. This is in practice far from true, even at $R > 15{,}000$ when the cells appear visually to be very good hexagons. Conversely, near critical, the cells appear to be almost perfect rectangles, yet the term $(0, 2)$ which should be zero for a pure rectangle so inclined to the axes is still present. Similarly the first overtone of a pure hexagon has wave-number $a\sqrt{3}$ and consists of the terms $(2, 0)$ and $(1, 3)$. As in the two-dimensional single cell results, this first harmonic is strongly present. Also given are the amplitudes of the second harmonic (with wave-number $2a$) comprising the terms $(2, 2)$ and $(0, 4)$ and the first overtone with a toroidal part (not, of course, present in the vertical component), which has wave-number $a\sqrt{7}$ and has the three components $(1, 5)$, $(2, 4)$ and $(3, 1)$.

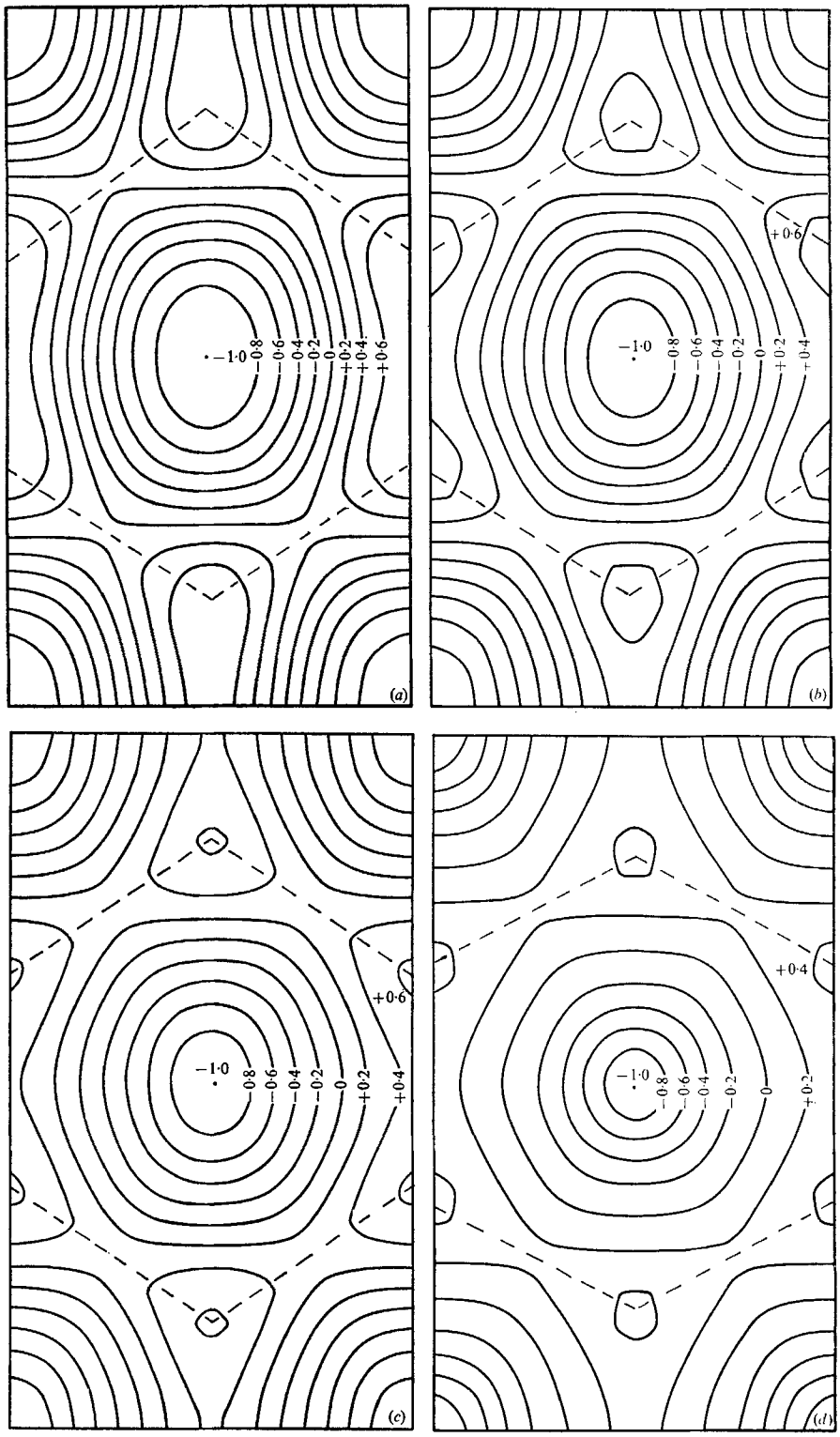

FIGURE 4. Iso-lines of vertical velocity normalized to unity at the centre with cell boundaries indicated approximately by broken lines. $P = 6{\cdot}8$, $a = 2{\cdot}63$. (*a*) Rayleigh number 4000. (*b*) Rayleigh number 8000. (*c*) Rayleigh number 10,000. (*d*) Rayleigh number 20,000.

The amplitudes of higher terms are not reliable in view of the small grid sizes involved. (For a discussion of significance and form of the poloidal and toroidal overtones see Ehrenzweig (1969).) In each of the above calculations a downward hexagonal initial perturbation leads to a cell with downward central motion. In calculations with upward initial perturbations the flow rapidly reversed in sign and the final steady solutions were indistinguishable from the corresponding ones with downward initial states.

The values of M obtained for various Rayleigh numbers are given in table 4 as a function of grid size along with the 'best' estimates of M for rolls from table 2. An additional column here gives M calculated for roll solutions obtained with the three-dimensional programme. These are given only for comparison since only 4 points were used to represent their co-axial direction and therefore nothing can be said of their stability to disturbances in this direction. The three-dimensional cells have M values consistently larger than those from the two-dimensional programme, but, in view of the grid-size dependence shown here and in table 2, this difference can hardly be considered significant. The calculations were discontinued when the values of M and N had reached steady values in the manner described in § 3.1 for rolls.

Calculations with values of λ large enough to permit a number of three-dimensional cells to co-exist must await a much larger and faster computer, but some attempts were made to increase λ from λ_c to about $3\lambda_c$. This produced behaviour reminiscent of that of the two-dimensional analogue. The single cell broke into a composite one which appeared to be mainly the first natural harmonic at $\lambda \simeq 1{\cdot}5\lambda_c$. One example of such a state appears in table 3, case 4. Reversing the process, reducing λ back to λ_c caused the original planform to be recovered with a large hysteresis in λ.

3.3. *Low Prandtl numbers*

With P of unity, the behaviour differed considerably from that described above. For R greater than about $2R_c$, all hexagonal perturbations, of either sign, produced rolls, in the y direction for an R of less than 10,000 (wave-number $\frac{1}{2}\sqrt{3}\,a$) and in the x direction for higher R (wave-number a). This again tends to indicate a decrease of preferred wavelength on increasing R. In the range $R_c < R < 2R_c$, the solutions resembled those for higher values of P, being basically rectangular in planform. Some integrations were also attempted in which, with $\lambda = \lambda_c$ and $R = (8000, 10{,}000, 12{,}000)$, P was steadily decreased from 6·8 to 1·0; the expected change from three- to two-dimensional flow occurred at $P \sim 2{\cdot}5$ irrespective of the chosen value of R.

4. Discussion

For all the Rayleigh numbers, R, and Prandtl numbers, P, considered in this paper, some form of tessellated solution of the non-linear equations is found, provided that R exceeds the critical value R_c.

No convective solutions were found for $R < R_c$, although attempts were made to initiate such solutions by means of perturbations of considerable amplitude in the form of both up and down hexagons, rectangles and rolls. This is rather

				Values of a' and (s,t)								
				a		$a\sqrt{3}$		$2a$		$a\sqrt{7}$		
Case	R	λ	a	(1, 1)	(0, 2)	(1, 0)	(1, 3)	(2, 2)	(0, 4)	(1, 5)	(2, 4)	(3, 1)
1	5000	2·39	2·63	−0·2641	−0·0829	+0·0229	−0·0327	+0·0055	+0·0035	−0·0015	−0·0026	−0·0049
2	10,000	2·39	2·63	−0·4686	−0·2508	+0·0047	+0·0609	−0·0094	+0·0172	−0·0053	−0·0148	−0·0236
3	15,000	2·39	2·63	−0·5865	−0·4110	−0·0146	−0·0396	−0·0335	+0·023	−0·0087	−0·0354	−0·0427
4	10,000	4·46	1·4	−0·1466	−0·0931	+0·2494	+0·2850	+0·2912	+0·0925	−0·0231	+0·0006	+0·0182

TABLE 3. (x, y) Fourier components of the vertical, mid-depth, velocity distribution. Each term is of the form $\cos(\frac{1}{2}\sqrt{3}\,sax)\cos(\frac{1}{2}tay)$. The total wave-number of each harmonic, a', is $\frac{1}{2}a(3s^2+t^2)^{\frac{1}{2}}$

surprising since, in a possibly analogous situation, Krishnamurti (1969) found subcritical up hexagon solutions both by experiment and theory. Busse (1967*a*) found subcritical hexagons in the case of Bénard convection where the fluid had varying material properties. Presumably, if such a region of subcritical hexagons exists, it is too narrow to be found by this type of three-dimensional analysis. For R between R_c and about $2R_c$ the general planform and cell structure is largely independent of P. This is to be expected since the linear theory is P independent. In this region the cells are three-dimensional and mainly rectangular in appearance. At larger values of R, the planform depends on the value of P. If this is of order unity (in particular, less than about 2·5), the only planform found is the roll. If P is above this range, three-dimensional cells persist, their shape depending on R, becoming progressively more hexagonal as R increases until, for R above about $5R_c$, they appear to be almost perfect hexagons.

	Polygons			Rolls	
$R \times 10^{-3}$	$12 \times 12 \times 13$	$20 \times 20 \times 9$	$20 \times 20 \times 13$	$20 \times 4 \times 13$	40×33
3	1·05	**	1·05	1·05	1·05
4	1·20	**	1·23	1·23	1·20
5	1·35	**	1·38	1·34	1·35
8	1·66	**	1·71	1·70	1·65
10	1·83	1·90	1·87	1·84	1·80
15	2·11	2·14	2·15	2·11	2·05

TABLE 4. Values of the parameter M for various grid sizes and Rayleigh numbers at $P = 6{\cdot}8$

On the question of wave-number, only small values of λ were used in the three-dimensional calculations because of the limitations of computer time and storage. Thus only approximate bounds for this quantity can be given. The results, however, are adequate to demonstrate that a typical cell will break into its first overtone if λ exceeds about $1{\cdot}5\lambda_c$. Such planform transitions are always associated with an increase in M as is also the splitting of one cell into two or three when λ exceeds $2\lambda_c$ in two dimensions. This might encourage the heuristic belief that some particular wave-number is naturally selected which maximizes M or some similar property of the motion. On the other hand, in the large λ results, the most common wavelength is not that which would maximize M. Similar attempts to establish an extremum principle for Bénard convection have been similarly unsuccessful. The experimentally observed wave-numbers differ consistently by several per cent from the calculated values for maximum Nusselt number (see Somerville 1969). Busse's (1967*b*) results also suggest that a range of stable wave-numbers exists for moderate values of R.

The configuration considered in this study differs essentially from Bénard convection in that the temperature boundary conditions are asymmetric and the static equilibrium temperature profile is parabolic rather than linear. Theoretical calculations by Palm (1960) and later by Segel & Stuart (1962) in which this symmetry is removed by the inclusion of a temperature-dependent viscosity,

showed that the direction of motion of the centres of hexagonal cells followed the direction of decreasing viscosity. An equivalent result was obtained by Krishnamurti (1969), with a Bénard-like physical system having uniform viscosity but with time-varying boundary temperatures. Here the direction of flow was in the direction of decreasing gradient of the static temperature profile with depth. In the internally heated situation this rule would predict that only downward polygons are possible, as has been found in this study. Roberts's theory and both Tritton & Zarraga's and Hooper's experiments also agree on this point, although they seem to be in conflict at low Rayleigh numbers. Roberts's conclusion that only rolls are stable for R less than a Prandtl-number-dependent critical value

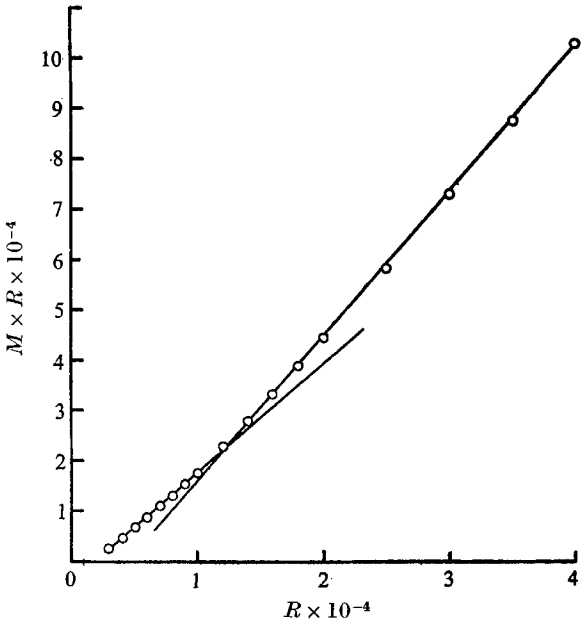

FIGURE 5. The product $M \times R$ as a function of R showing slope change at $R \sim 12{,}000$.

($\simeq$ 8750 for water) was, presumably, due to the erroneous exclusion of rectangular-type cells from his calculations. Segel & Stuart did consider this type of cell, and found that it was the only stable form of three-dimensional cell provided the temperature variation of viscosity was small enough, otherwise hexagons were more stable. This suggests that the relatively large viscosity variations present in Tritton & Zarraga's apparatus could account for all their cells being hexagonal. Busse's (1967*a*) stationary equations appear to exclude such planforms, however. Perhaps our restriction of the horizontal periods to be always in the ratio of $1:\sqrt{3}$ is significant here? Hooper reports polygonal cells for all R but also that a discontinuity of slope occurs in a plot of the product $M \times R$ against R at about $R = 11{,}000$. This could represent some change in cell structure at this Rayleigh number. A similar plot using calculated values of M as given in figure 5 shows a similar effect.

The most curious property of Tritton & Zarraga's results is the enormous increase in cell size with Rayleigh number. This is not wholly confirmed by Hooper whose cells increase less rapidly in size with R. The results of the calculation in this paper still seem to support Roberts's view that cell sizes decrease with increased R, although the evidence for this is mainly from roll solutions. It was not however possible to create down hexagons of a size consistent with Tritton & Zarraga's results as such solutions always split into their first overtone. These considerable differences of cell size between experiment and calculation could be due to the idealized mathematical model of the latter not representing the physical configuration of the former in some way. In particular, variations in the, assumed constant, temperature of the upper surface of the layer might be significant. A closely related problem which could be regarded as an extreme case of such variation, in which the upper surface condition has been replaced by one of constant heat flux, has been studied by Jakeman, Hurle & Pike (1967).

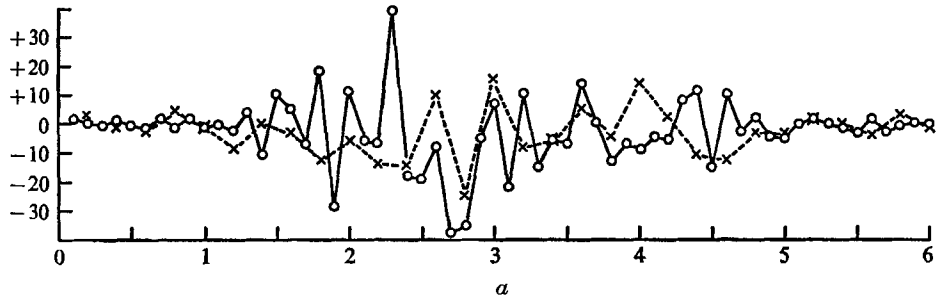

FIGURE 6. Fourier harmonics of vertical velocity at $R = 10{,}000$, $P = 6{\cdot}8$ with constant heat flux boundary conditions in top surface. – – × – –, wavelength 10π; —○—, wavelength 20π.

Their linear stability analysis shows that the critical Rayleigh number is considerably reduced by this change, and that the critical wave-number becomes zero. (This corresponds to a cell of infinite wavelength !) This raises the possibility that any imperfection in the uniformity of cooling of an experimental apparatus might enlarge the cells. To examine such a situation, the boundary condition (5) has to be replaced by

$$\partial T/\partial z = -1 \quad \text{and} \quad \mathbf{u} = 0 \quad \text{on} \quad z = 1,$$

and a new zero point on the temperature scale provided by insisting that $\langle T \rangle = 0$ on $z = 1$. Figure 6 shows the Fourier decomposition of the resulting vertical velocities for two-dimensional runs otherwise comparable to those of figure 3. The initial conditions were $\lambda = 10\pi$ and 20π, $R = 10{,}000$ and $P = 6{\cdot}8$, with a single cell perturbation to initiate the motion. The dominant wavelengths are considerably greater than those of figure 3. There is also a noticeable tendency for subharmonics to persist. It must, however, be borne in mind that with an experimental fluid consistency mainly of water, and a good conducting metal plate on top of their apparatus, spatial variations in Tritton & Zarraga's surface temperature must have been small.

One other experimental limitation that would influence cell size is that due to the use of rigid end walls. Figure 7 shows the Fourier decomposition of one test

iteration in two dimensions with $\lambda = 10\pi$, $R = 10{,}000$ and $P = 6{\cdot}8$ in which the usual cyclic conditions were replaced by rigid end walls. Comparison with the otherwise identical case in figure 3 reveals little change either in the range of wave-numbers present, or in the absence of significant sub- or supercritical harmonics. In three dimensions the situation is less clear. The Fourier spectra of the only multiple cell integrations available are typified by table 3, case 4. This shows a large contribution from the first subcritical harmonic. The limited finite difference accuracy of such three-dimensional results may account for this. This aspect, along with better estimates of the preferred wave-numbers of hexagonal/rectangular cells must await either qualitative physical experiments with layers of variable horizontal size or numerical simulations capable of producing many adjacent cells.

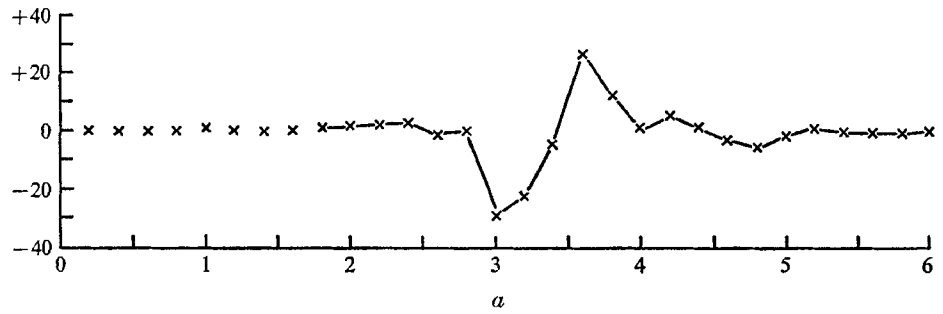

FIGURE 7. Fourier components of vertical velocity at $R = 10{,}000$, $P = 6{\cdot}8$ and $\lambda = 10\pi$ with normal boundary conditions on top surface but rigid boundary conditions replacing the periodic boundary conditions on the sides of the layer.

This study was made practicable by the generous provision of computer time, initially by the U.K.A.E.A., Culham Laboratory, and latterly by the University of Newcastle Computing Laboratory, to whose Director, Professor E. S. Page, I am particularly indebted. Figures 4 (*a*), (*b*), (*c*) and (*d*) were drawn on an IBM 1627 graph plotter kindly made available by Newcastle Polytechnic. Our thanks are also due to Dr A. Chorin for the supply of copies of his computer programmes, to Dr D. C. Tozer and Dr D. J. Tritton for some interesting discussions and to Professor P. H. Roberts, at whose suggestion the study was undertaken.

REFERENCES

BUSSE, F. 1967*a* *J. Fluid Mech.* **30**, 625.

BUSSE, F. 1967*b* *J. Maths. Phys.* **46**, 140.

CHANDRASEKHAR, S. 1961 *Hydrodynamic and Hydromagnetic Stability.* Oxford University Press.

CHORIN, A. 1967*a* *J. Comp. Phys.* **2**, 12.

CHORIN, A. 1967*b* *Bull. Am. Math. Soc.* **73**, 928.

DEBLER, W. R. 1966 *J. Fluid Mech.* **24**, 165.

DOUGLAS, J. 1962 *Numerische Math.* **4**, 41.

EHRENZWEIG, P. 1969 *Quart. J. Mech. App. Math.* **22**, 355.

FROMM, J. E. 1965 *Phys. Fluids*, **8**, 1757.

HARLOW, F. H. & WELCH, J. E. 1965 *Phys. Fluids*, **8**, 2182.

JAKEMAN, E., HURLE, D. T. J. & PIKE, R. E. 1967 *Proc. Roy. Soc.* A **296**, 469.

KRISHNAMURTI, R. 1969 *Geophys. Fluid Dynamics Inst. Florida State Univ. Tech. Report* no. 14.

PALM, E. 1960 *J. Fluid Mech.* **8**, 183.

PEACEMAN, D. W. & RACHFORD, H. H. 1955 *J. Soc. Industr. Math.* **3**, 28.

PEARSON, J. R. A. 1958 *J. Fluid Mech.* **4**, 489.

PEARSON, J. R. A. 1964 *Sperry Rand Research Centre, Sudbury, Mass. Report* no. SRRC-RR-64-17.

PLOWS, W. H. 1968 *Phys. Fluids*, **11** 1593.

ROBERTS, P. H. 1967 *J. Fluid Mech.* **30**, 33.

ROSSBY, H. T. 1969 *J. Fluid Mech.* **36**, 309.

SAMARSKIĬ, A. A. 1963 *U.S.S.R. Comp. Math. and Math. Phys.* **5**, 894.

SCHLÜTER, A., LORTZ, D. & BUSSE, F. 1965 *J. Fluid Mech.* **23**, 129.

SEGEL, L. A. & STUART, J. T. 1962 *J. Fluid Mech.* **13**, 289.

SOMERVILLE, R. C. J. 1969 To appear.

STUART, J. T. 1958 *J. Fluid Mech.* **4**, 1.

TRITTON, D. J. & ZARRAGA, M. N. 1967 *J. Fluid Mech.* **30**, 21.